Evaluation Of Velocity-Sensitised And Acceleration-Sensitised NCE-MRA For Below-Knee Peripheral Arterial Disease

Shaida N[1] MBBS FRCR, Priest AN[2] PhD, See TC[1] MBBS FRCR, Winterbottom AP[1] MBBS FRCR, Graves MJ[2] PhD, Lomas DJ[3] MB B Chir FRCR

[1] Department of Radiology, Addenbrooke's Hospital, Cambridge UK

[2]Department of Medical Physics, Addenbrooke's Hospital, Cambridge UK

[3]Academic Department of Radiology, University of Cambridge, UK

Corresponding author: Nadeem Shaida, Department of Radiology, Box 218, Addenbrooke's Hospital, Hills Road, Cambridge CB2 0QQ Tel: 01223 245 151 x 2337 Email: nadeem.shaida@addenbrookes.nhs.uk

Grant Support: The authors gratefully acknowledge financial support from the Addenbrooke's Charitable Trust and the NIHR Cambridge Biomedical Research Centre.

Running Title: NCE-MRA for below knee disease

Abstract

Purpose: To evaluate the diagnostic performance of velocity- and acceleration-sensitized non-contrast enhanced magnetic resonance angiography (NCE-MRA) of the infrageniculate arteries using contrast-enhanced MRA (CE-MRA) as a reference standard.

Materials & Methods: 24 patients with symptoms of peripheral arterial disease were recruited. Each patient's infrageniculate arterial tree was examined using a velocity-dependent flow-sensitized dephasing (VEL-FSD) technique, an acceleration-dependent (ACC-FSD) technique and our conventional CE-MRA technique performed at 1.5T. The images were independently reviewed by 2 experienced vascular radiologists, who evaluated each vessel segment to assess visibility, diagnostic confidence, venous contamination and detection of pathology.

Results: 432 segments were evaluated by each of the 3 techniques by each reader in total. Overall diagnostic confidence was rated as moderate or high in 98.5% of segments with CE-MRA, 92.1% with VEL-FSD and 79.9% with ACC-FSD. No venous contamination was seen in 96% of segments with CE-MRA, 72.2% with VEL-FSD and 85.8% with ACC-FSD. Per-segment, per-limb and per-patient sensitivities for detecting significant stenotic disease were 63.4%, 73% and 92% respectively for ACC-FSD, and 65.3%, 87.2% and 96% for VEL-FSD, and as such no significant statistical change was detected using McNemars chi squared test with p-values of 1.00, 0.13 and 0.77 obtained respectively.

Conclusions: Flow-dependent NCE-MRA techniques may have a role to play in evaluation of patients with peripheral vascular disease. Increased sensitivity of a velocity-based technique compared to an acceleration-based technique comes at the expense of greater venous contamination.

Keywords: Magnetic Resonance Angiography, Blood Flow Velocity, Acceleration, Peripheral Arterial Disease, Peripheral Vascular Diseases

Introduction

Peripheral Arterial Disease (PAD) is a condition with increasing prevalence in the western world which has a significant impact on individual patients in terms of morbidity and mortality and on the wider health community as a whole [1]. Treatment options include lifestyle and medical measures along with surgical and increasingly endovascular procedures. Diagnostic imaging plays an important role in directing management with Duplex Ultrasound (DUS), CT Angiography (CTA) and Contrast Enhanced –Magnetic Resonance Angiography (CE-MRA) all being well established techniques [2]. These imaging modalities each have their own strengths and weaknesses. DUS has the advantage of being inexpensive, and being readily available. However its effectiveness is reduced in obese patients and in the assessment of the supra-inguinal arteries, particularly in the presence of bowel gas. In addition, operator dependency remains an important limitation in its utility. CTA provides an excellent overview of the vascular system, however it employs ionising radiation and the relatively high prevalence of renal impairment [3] in this cohort of often elderly arteriopaths means the use of intravascular contrast medium is often contra-indicated. In addition, accurate assessment of the small vessels below the knee, which are often heavily calcified, may prove challenging with CTA [4]. CE-MRA avoids the limitations of reduced effectiveness in the supra-inguinal region and the use of ionizing radiation. However, the use of gadolinium-based agents in CE-MRA has been implicated in the development of Nephrogenic Systemic Fibrosis (NSF) for patients with impaired renal function [5]. More recently, concerns have been raised regarding the accumulation of excess Gadolinium within the brain [6].

Given the limitations of each of the conventionally employed imaging modalities, it is no surprise that in recent years attention has turned to the development of Non-Contrast-Enhanced Magnetic Resonance Angiography (NCE-MRA) for evaluation of the peripheral vasculature. In addition to negating concerns regarding NSF, NCE-MRA also avoids the issue of resolution limitations during first

pass acquisition. Additionally, it does not require careful timing of the acquisition relative to a bolus passage, and can bring increased flexibility, for example allowing repeated acquisitions. Over time, original non-contrast techniques such as time of flight imaging have fallen out of favor for body imaging due to longer imaging times and concerns regarding image quality [7]. A number of newer techniques have been described which rely on intrinsic properties of flowing blood, such as relaxation times or flow characteristics [8-13]. It is important that such methods are evaluated against existing techniques as a standard, with promising results already seen using a number of different techniques [14-16].

One recently developed NCE-MRA method uses a subtraction-based technique, combined with a controllable flow-dependent preparation module which suppresses the signal from flowing blood [13,17]. A "dark blood" image is produced which can be subtracted from a non-flow-suppressed "bright blood" image to produce an image of the vasculature. By adjusting the strength of the motion sensitization gradients (MSG), the flow suppression can be adjusted such that visualisation of the arteries, veins or both is optimised. This technique is known either as 'Flow-Sensitized Dephasing' (FSD) or as 'Vascular Anatomy by Non-Enhanced Static Subtraction Angiography' (VANESSA), and has previously been used to visualise the infrageniculate vessels [18]. More recently, it has been demonstrated in healthy volunteers that the use of an acceleration-dependent flow-suppression module (then referred to as 'ADVANCE-MRA') rather than a velocity-dependent flow-suppression module can improve arterio-venous separation, due to the intrinsic pulsatility of arterial flow [19]. The objective of this study was to compare the diagnostic and qualitative performance of the acceleration- and velocity-sensitized techniques in a population of patients with peripheral arterial disease, using our standard CE-MRA technique (Time-resolved imaging of contrast kinetics – TRICKS) as a reference standard. In this work, the velocity-sensitized FSD method will be known as VEL-FSD and the acceleration-sensitized method as ACC-FSD.

Materials and methods

The study was approved by the local ethical committee and written informed consent was obtained from all patients. 24 patients with symptoms of peripheral arterial disease were recruited following referral for routine contrast enhanced MRA.

Pulse sequences and scan protocols

The MRI examinations were performed using a 1.5 T MR system (Signa HDx, GE Healthcare, Waukesha, WI) with an 8-channel cardiac array coil. The 2 non-contrast methods under investigation were performed initially, followed by the routine CE-MRA. Scan triggering was performed using pulse oximetry. In order to locate the major leg arteries, an initial axial multi-slice 2D time of flight (TOF) acquisition was acquired, with the following scan parameters: echo time (TE) 1.4 ms; repetition time (TR) 4.9 ms; flip angle 60°; acquired matrix 256×96; field of view (FoV) 33×25cm^2; slice thickness 5 mm; 84 slices. This was followed by a single-slice axial 2D cine phase-contrast acquisition through the popliteal arteries below the knee (TE 3.7 ms; TR 7.1 ms; flip angle 30°; acquired matrix 256×64; field of view (FoV) 28×14 cm^2; slice thickness 5 mm; velocity encoding parameter (venc) 50–70 cm/s; retrospective gating with 100 reconstructed phases over the cardiac cycle). This was used to assess quickly the pulsatility of flow and the approximate time of peak arterial flow within the cardiac cycle (using the scanner's 'FuncTool' software), in order to set the trigger delay for the subsequent NCE-MRA. If peak flow times varied between the two legs, the used setting aimed for the best compromise to aim for flow suppression in both legs if possible.

Non-contrast-enhanced MRA was acquired using two subtraction-based methods, whose flow-preparation modules are shown in Fig. 1—the velocity-dependent method VEL-FSD, which for this study used an iMSDE module [20] for flow suppression (Fig. 1a) and the acceleration-dependent

method ACC-FSD (Fig. 1b). Note that these two flow-suppression modules differ mainly in the signs of the motion-sensitization gradients (MSG).

Each NCE-MRA method used balanced steady-state free precession (bSSFP) for the imaging readout, with the following acquisition parameters: TE 1.6 ms, TR 3.5 ms, flip angle 65°, acquisition matrix 256×224×28, FoV 33.3×30.0 cm, slice thickness 2.4 mm, oblique coronal orientation. For each 3D NC-MRA sequence, scan time was 60 beats per volume, or 300 beats for the 5 volumes acquired. This corresponds to 5 minutes at a heart rate of 60bpm.

Parallel imaging (regularized ASSET) was used with an acceleration factor of 2. The reconstructed resolution was increased by a factor of 2 in all three directions using zero-fill interpolation. Fat-saturation was applied twice: before the flow-preparation modules, to avoid stripes in the flow-suppressed image [17]; and before the image readout, to reduce the fat signal in the images.

For flow-suppression, the ACC-FSD acquisition used an acceleration-preparation module with an effective echo time (TE_{eff}) of 50 ms. In addition to a bright-blood image, four dark-artery images were acquired using MSG with duration 8 ms and amplitudes 0.5, 1.0, 2.0 and 5.0 mT/m. This results in acceleration-encoding parameters (aenc) of 8.96, 4.48, 2.24 and 0.896 m/s^2 respectively [19]. For both bright- and dark-blood images, the flow-sensitization module was placed at the time of peak arterial flow as determined from the phase-contrast measurements, in late systole. Following the flow-suppression module, there was a delay of 200ms delay before the readout. This delay was added to place the readout in the diastolic portion of the cardiac cycle and thus avoid the reductions in vascular image quality that can occur due to rapid inflow into the image volume during the readout [18], and its duration was chosen based on typical flow profiles seen in volunteers and previous patients during initial testing. For this dataset, the five image volumes were acquired consecutively in a single acquisition with automatic adjustment of the MSG amplitudes, and the only protocol adjustments needed from the operator were to define the image geometry and the time of peak flow.

The VEL-FSD acquisition used an iMSDE module with TE_{eff} 30 ms. One bright-blood and four dark-blood images were collected using MSG with duration 3.4 ms and amplitudes of 0.5, 1.0, 2.0 and 15.0 mT/m. This corresponded to velocity-encoding parameters (venc) of 23.0, 11.5, 5.76 and 0.768 cm/s respectively. The final 15.0 mT/m acquisition gave images showing both arteries and veins. For the dark-blood images, the flow-sensitization (iMSDE) module was placed at peak arterial flow, but for the bright-blood image a delay of 300 ms was added to place it in diastole. There was no additional delay between flow-sensitization module and the readout. As above, the five image volumes were acquired consecutively in a single acquisition, with the operator defining only the image geometry and the time of peak flow.

The NCE-MRA acquisitions were followed by our standard clinical CE-MRA protocol using TRICKS, with the following scan parameters: TE/TR 2.8/8.3 ms; flip angle 45°; FoV 44×30 cm^2; acquired matrix 512×156×28; slice thickness 2.4 mm. This gives an acquired spatial resolution of 0.86×1.92×2.40 mm^3. The total scan time for a mask phase and 10 dynamic phases was 170 seconds, with a temporal resolution of 10.5 seconds and a temporal footprint of 63 seconds. A dose of 10 ml Gadobutrol (Gadovist, Schering AG) was given, followed by a 20 ml saline flush, at a rate of 0.5 ml/second. The orientation, thickness and (approximate) position of the imaging slices were matched for the CE- and NCE-sequences.

Assessment

To remove the edge regions most commonly affected by signal loss due to magnetic field inhomogeneity, the NCE-MRA images were cropped by 30 pixels in the S and I directions, giving a final S/I FoV of 29.4 cm. The CE-MRA images were then cropped in the S and I directions to a precisely matched FoV, to ensure that the same regions were compared in the subsequent comparisons.

The images were then assessed independently by two vascular radiologists with 8 and 4 years experience respectively (TCS and APW). For both the CE-MRA and the NCE-MRA datasets, multiple phases/image volumes were available for assessment and reviewer was able to choose the 'best' phase for assessment. Overall 432 segments were evaluated for each of the 3 techniques by each of the two reviewers. The reviewers were blinded to patient identity and the examinations were reviewed in a semi-randomised order, with care taken to ensure that the datasets for any given patient were not assessed in close temporal proximity. For analysis purposes the data from each reviewer were treated as separate data-points, given that the purpose of the study was to compare the two non-contrast techniques with CE-MRA as the reference standard.

Both MIPs and individual slices were available for assessment. The below-knee arterial station was divided into 9 segments: the proximal and distal below-knee popliteal (Pop), the tibio-peroneal trunk (TPT), the proximal and distal anterior tibial (AT), proximal and distal peroneal artery and the proximal and distal posterior tibial (PT) arteries. To ensure equivalence between the 2 readers the boundary between proximal and distal segments of vessels was defined as the mid point of the vessel length assuming it continued to the edge of the field of view (ie. inferiorly for the AT, peroneal and PT and superiorly for the popliteal artery). For each of the 3 techniques, each vessel segment was assessed in three separate ways. Firstly the vessel visibility was assessed as either visible (y), not visible (n), or partially visible (p). For partially or not visible segments, it was judged whether this related to pathology or to the imaging technique. This was left to the discretion of the expert reader although as a guide it was suggested that signal loss which either affected the edges of the image, with good signal in other arteries, or which affected a wide central region, was deemed as "technique related" if no collateral vessels were present to suggest disease. Then, diagnostic confidence was assessed on a four-point Likert scale (non-diagnostic, low confidence, moderate confidence and high confidence). Finally, the venous contamination was assessed on a three-point scale, none (0), some - but not affecting diagnosis (1) and significant - affecting diagnosis (2).

Diagnostic confidence was then differentiated into moderate or high confidence versus low confidence or non-diagnostic for analysis purposes. Each segment was also assessed for pathology in terms of being normal, stenosis <50%, stenosis>50% or occlusion. From the disease evaluation, the sensitivity, specificity, positive predictive value (PPV) and negative predictive value (NPV) for detection of significant stenosis (>50%) were evaluated, considering CE-MRA as the reference standard. Non-evaluable segments on NCE-MRA that were visible on TRICKS were counted as "misses" for the purposes of evaluating sensitivity. In order to detect a difference in sensitivity between the two tests under consideration, the McNemar Chi-squared test was used. This was calculated on a per-segment, per-limb and per-patient basis. Given the small numbers in the per-limb and per-patient basis, Yates correction of 0.5 was applied. All statistical analysis was done using Microsoft Excel.

Results

A total of 24 patients (17 male and 7 female, mean age 64.9 years, range 55–80yrs) with symptoms of peripheral vascular disease were recruited, following referral for routine contrast-enhanced peripheral MR angiography. Of the study group, the majority of patients had claudication (Rutherford 1-3), although 2 patients had rest pain (Rutherford 4) and one patient had tissue loss (Rutherford 5). The complete breakdown of the claudication patients was 3 with Rutherford 1, 12 patients with Rutherford 2 and 6 patients with Rutherford type 3 disease.

Figure 2 shows typical representative images obtained for three example patients using the 3 different techniques. The phase-contrast velocity profiles are shown for comparison, to demonstrate that for each of these cases there is some pulsatility of flow in both legs, even though the flow profiles may differ substantially between them.

Figure 3 shows the results for segment visibility out of a possible total of 864 segments for each technique. This demonstrates overall better visibility of segments using the VEL-FSD technique as compared to the ACC-FSD although neither performed as well as the CE-MRA standard. Of the 256 segments (out of 864) graded as not visible or partially visible using ACC-FSD, 205 segments (80.0%), and of the 157 segments graded as not visible or partially visible using VEL-FSD, 75 segments (47.8%) were thought to be due to technique-related issues rather than due to occlusive pathology. Concordance between the two reviewers regarding whether a segment was not visible due to technique or pathology was 50% for the ACC-FSD, 36.2% for VEL-FSD and 55.6% for CE-MRA.

Overall diagnostic confidence was rated as moderate or high in 98.5% of segments scored using CE-MRA, 79.9% using ACC-FSD and 92.1% using VEL-FSD. Table 1 shows the diagnostic confidence of each method by segment. The sensitivity, specificity, PPV and NPV of the two methods using CE-MRA as the gold standard and considering stenosis >50% as significant disease on a per segment, per limb and per patient basis is shown in Table 2. McNemar's Chi-squared test did not demonstrate significant difference in sensitivity for significant stenosis between the two techniques on a per-segment ($p=1.00$), per-limb ($p=0.13$) or per-patient ($p=0.77$) basis, although the per limb results came closest to reaching significance.

The degree of venous contamination (Figure 4) was scored as none in 96% of evaluated segments using CE-MRA as compared to 85.8% using ACC-FSD and 72.2% using VEL-FSD. The respective percentage scores for some venous contamination were 3.5%, 11.9% and 23.3% and for significant venous contamination 0.5%, 2.3% and 4.5%.

It was noted that in four cases, the phase contrast flow profiles showed little or no flow pulsatility for one of the legs, and that this corresponded with a poor signal in acceleration-sensitized NCE-MRA for the corresponding leg. Two examples are shown in Figure 5.

Discussion

The aim of this study was to explore the use of novel non-contrast MRA techniques for the evaluation of the infregeniculate vessels in patients with PAD. The infrageniculate arteries pose a challenging imaging problem by conventional imaging modalities due to the small size of the vessels and the presence of calcification hampering assessment by CTA and DUS. Nevertheless, as techniques both by open surgery and in particular by endovascular means improve, stenoses and occlusions in these vessels that were once untreatable are now being routinely revascularised. The emergence of the angiosome concept in targeting revascularisation [21] means accurate pre-procedure imaging is key in planning intervention. Better MRA reconstruction algorithms recently have led to an improvement in spatial resolution and quality [22,23] In addition, a number of NCE-MRA techniques have also been described of which some are flow-independent [24] and others rely on the inherent properties of flowing blood [25-27]. Most of these studies have demonstrated technical feasibility although real-world data in specific at-risk population groups such as diabetic patients remains limited [28]. Newer developments such as examinations performed at 3T hold promise for the future [29,30].

This work assessed two recently-developed flow-dependent subtraction-based methods of performing NCE-MRA: the VEL-FSD technique, which has previously been demonstrated [15] to provide visibility of the infrageniculate vessels in patients with PAD, relies on the velocity of blood; and ACC-FSD, which relies on acceleration and has been shown to provide beneficial artery-vein separation in healthy controls [16]. This study compares the two methods when used for assessment of the infrageniculate vessels, with CE-MRA as a reference standard. We have demonstrated that overall visualisation of the various infrageniculate segments is reasonable with both techniques when compared to CE-MRA. The experienced reporters felt more comfortable in terms of diagnostic confidence using VEL-FSD rather than ACC-FSD. Overall per-patient sensitivity to disease is high for both techniques, although the per-segment sensitivity is considerably lower. This is not entirely

unsurprising given that multifocal disease is common in this patient cohort Another contributory factor could be related to technique failure near the edge of the field of view although previously similar reported issues with vessel visualisation are less evident with the current version of the VEL-FSD method.As expected the ACC-FSD technique is more resistant to venous contamination than VEL-FSD.

Examination of the flow profiles measured by phase contrast MR helps us to better understand some of the strengths and weaknesses of these flow-dependent NCE-MRA techniques. These profiles were used to align the timing of the flow-suppression modules with peak arterial flow. However in some cases the flow profiles for the two legs differed substantially and it was not possible to find a delay time which was optimal for both legs simultaneously and in these situations the chosen timings aimed to allow flow suppression in both legs as far as possible. Future work might improve this by performing either the flow-sensitization or the entire imaging process for the two legs separately in such cases, so that each leg could be optimised independently.

In many cases, the flow profiles measured in the below-knee arteries were adversely affected by proximal disease in the above-knee vessels. Flow velocities were typically much lower than those seen in healthy volunteers. The flow profiles also revealed that in some cases, there was little or no flow acceleration in legs with severe upstream stenoses. In such cases, the vessels were poorly depicted by the ACC-FSD sequence. Thus, ACC-FSD is probably unsuitable for reliable clinical imaging in such cases. However, ACC-FSD may still have other beneficial uses: it is useful in mapping normal anatomy without venous contamination, and in some clinical situations it may be a useful addition to VEL-FSD to aid the discrimination of arteries and veins, which are not always separated by this technique. Since both VEL-FSD and ACC-FSD may be acquired using the same bright-blood images, a combined VEL/ACC-FSD sequence could be acquired with a relatively small increase in the overall scan time.

Both NCE-MRA methods used bSSFP as the readout method. The sensitivity of this method to off-resonance effects does limit its success in the lower extremities, especially given the relatively poor homogeneity of the main magnetic field often achieved in this region. Such off-resonance effects limit the useful maximum FoV of the method, which may account for the lower performance of these methods compared to CE-MRA. In future, it is hoped that alternative readout strategies will improve the underlying image quality and thus improve diagnostic performance.

Other limitations of the study include the relatively small number of patients studied although it is anticipated that as the techniques become more refined, in the future larger patient populations with specific at-risk subgroups such as diabetic patients will be studied. Both techniques described rely on assessment of flow in the popliteal and infrageniculate vessels, however only the infrageniculate vessels have been investigated here.

Ultimately, it may be the case that conventional imaging techniques (such as ultrasound or CT) may be employed for imaging of the larger ilio-femoral vessels with single-station below-knee NCE-MRA employed in situations where conventional techniques may not be optimal, for instance in the obese patient or in those with calcified vessles.. The infrageniculate region was chosen for analysis with the expectation that even better results would be achieved in the iliac or femoro-popliteal segments due to the larger size of the vessels. Another role for this techanique could be in patients with mixed arterial and venous leg ulcers where rapid arterio-venous shunting can limit the use of CE-MRA due to venous contamination. Potentially an algorithm whereby CE-MRA is employed in the supra-inguinal and femero-popliteal segments with NCE-MRA techniques below the knee could be considered.

Finally, CE-MRA has been used as the reference standard in line with most published studies in the literature [31]. It may be that digital subtraction angiography (DSA) is a more appropriate “gold standard” to compare with although clearly there may be practical and ethical issues in performing such a comparison.

Flow-dependent NCE-MRA techniques using acceleration and velocity flow sensitization may have diagnostic value in the assessment of patients with peripheral arterial disease. In this study comparing the initial diagnostic performance in such patients using both techniques, there was greater diagnostic confidence using the velocity sensitization approach (VEL-FSD) but at the expense of greater venous contamination.

References

1. Brevetti G, Chiariello M (2004) Peripheral arterial disease: the magnitude of the problem and its socioeconomic impact. Curr Drug Targets Cardiovasc Haematol Disord 4:199-208
2. Tang GL, Chin J, Kibbe MR (2010) Advances in diagnostic imaging for peripheral arterial disease. Expert Rev Cardiovasc Ther 8:1447-1455
3. Goldfarb S, McCullough PA, McDermott J, Gay SB (2009) Contrast induced –Kidney injury: Speciality specific protocols for interventional radiology, diagnostic computed tomography radiology and interventional cardiology. Mayo Clin Proc 84 (2): 170-179
4. Brockmann C, Jochum S, Sadick M, Huck K, Ziegler P, Fink C, Schoenberg SO, Diehl SJ (2009). Dual energy CT angiography in peripheral arterial occlusive dsease CVIR 32 (4): 630-637
5. Daftari Besheli L, Aran S, Shaqdan K, Kay J, Abujudeh H (2014) Current status of nephrogenic systemic fibrosis. Clin Radiol 69:661-668
6. Runge VM (2016). Safety of the gadolinium based contrast agents for MRI focusing in part on their accumulation in the brain and especially in the dentate nucleus. Invest Radiol 51 (5): 271-9
7. Ho KY. MR angiography of peripheral arteries (2004) JBR-BTR 87:46-49.
8. Miyazaki M, Takai H, Sugiura S, Wada H, Kuwahara R, Urata J (2003) Peripheral MR angiography: separation of arteries from veins with flow-spoiled gradient pulses in

electrocardiography-triggered three-dimensional half-Fourier fast spin-echo imaging. Radiology 227:890-896

9. Katoh M, Stuber M, Buecker A, Günther RW, Spuentrup E (2005) Spin-labeling coronary MR angiography with steady-state free precession and radial k-space sampling: initial results in healthy volunteers. Radiology 236:1047-1052
10. Koktzoglou I, Sheehan JJ, Dunkle EE, Breuer FA, Edelman RR (2010) Highly accelerated contrast-enhanced MR angiography: improved reconstruction accuracy and reduced noise amplification with complex subtraction. Magn Reson Med 64:1843-1848
11. Shimada K, Isoda H, Okada T et al. (2009) Non-contrast-enhanced hepatic MR angiography with true steady-state free-precession and time spatial labeling inversion pulse: optimization of the technique and preliminary results. Eur J Radiol 70:111-117
12. Edelman RR, Sheehan JJ, Dunkle E, Schindler N, Carr J, Koktzoglou I (2010) Quiescent-interval single-shot unenhanced magnetic resonance angiography of peripheral vascular disease: Technical considerations and clinical feasibility. Magn Reson Med 63:951-958
13. Fan Z, Sheehan J, Bi X, Liu X, Carr J, Li D (2009) 3D noncontrast MR angiography of the distal lower extremities using flow-sensitive dephasing (FSD)-prepared balanced SSFP. Magn Reson Med 62:1523-1532
14. Ward EV, Galizia MS, Usman A, Popescu AR, Dunkle E, Edelman RR (2013) Comparison of quiescent inflow single-shot and native space for nonenhanced peripheral MR angiography. J Magn Reson Imaging 38:1531-1538
15. Gutzeit A, Sutter R, Froehlich JM et al. (2011) ECG-triggered non-contrast-enhanced MR angiography (TRANCE) versus digital subtraction angiography (DSA) in patients with peripheral arterial occlusive disease of the lower extremities. Eur Radiol 21:1979-1987
16. Hodnett PA, Koktzoglou I, Davarpanah AH et al. (2011) Evaluation of peripheral arterial disease with nonenhanced quiescent-interval single-shot MR angiography. Radiology 260:282-293

17. Priest AN, Graves MJ, Lomas DJ (2012) Non-contrast-enhanced vascular magnetic resonance imaging using flow-dependent preparation with subtraction. Magn Reson Med 67:628-637
18. Priest AN, Joubert I, Winterbottom AP, See TC, Graves MJ, Lomas DJ (2013) Initial clinical evaluation of a non-contrast-enhanced MR angiography method in the distal lower extremities. Magn Reson Med 70:1644-1652
19. Priest AN, Taviani V, Graves MJ, Lomas DJ (2014) Improved artery-vein separation with acceleration-dependent preparation for non-contrast-enhanced magnetic resonance angiography. Magn Reson Med 72:699-706
20. Wang J, Yarnykh VL, Yuan C (2010) Enhanced image quality in black-blood MRI using the improved motion-sensitized driven-equilibrium (iMSDE) sequence. J Magn Reson Imaging 31:1256-1263
21. Söderström M, Albäck A, Biancari F, Lappalainen K, Lepäntalo M, Venermo M (2013) Angiosome-targeted infrapopliteal endovascular revascularization for treatment of diabetic foot ulcers. J Vasc Surg 57:427-435
22. Kramer H, Nikolaou K, Sommer W, Reiser MF, Herrmann KA (2009) Peripheral MR angiography. Magn Reson Imaging Clin N Am 17:91-100
23. Menke J (2010) Improving the image quality of contrast-enhanced MR angiography by automated image registration: a prospective study in peripheral arterial disease of the lower extremities. Eur J Radiol 75:e1-8
24. Cukur T, Lee JH, Bangerter NK, Hargreaves BA, Nishimura DG (2009) Non-contrast-enhanced flow-independent peripheral MR angiography with balanced SSFP. Magn Reson Med 61:1533-1539
25. Shin T, Hu BS, Nishimura DG (2013) Off-resonance-robust velocity-selective magnetization preparation for non-contrast-enhanced peripheral MR angiography. Magn Reson Med 70:1229-1224

26. Radlbauer R, Salomonowitz E, van der Riet W, Stadlbauer A (2011) Triggered non-contrast enhanced MR angiography of peripheral arteries: optimization of systolic and diastolic time delays for electrocardiographic triggering. Eur J Radiol 80:331-335
27. Mohrs OK, Petersen SE, Heidt MC, Schulze T, Schmitt P, Bergemann S, Kauczor HU (2011) High-resolution 3D non-contrast-enhanced, ECG-gated, multi-step MR angiography of the lower extremities: comparison with contrast-enhanced MR angiography. Eur Radiol 21:434-442
28. Liu X, Zhang N, Fan Z, Feng F, Yang Q, Zheng H, Liu P, Li D (2014) Detection of infragenual arterial disease using non-contrast-enhanced MR angiography in patients with diabetes. J Magn Reson Imaging 40:1422-1429
29. Knobloch G, Gielen M, Lauff MT, Romano VC, Schmitt P, Rick M, Kröncke TJ, Huppertz A, Hamm B, Wagner M (2014) ECG-gated quiescent-interval single-shot MR angiography of the lower extremities: initial experience at 3 T. Clin Radiol 69:485-491
30. Thierfelder KM, Meimarakis G, Nikolaou K, Sommer WH, Schmitt P, Kazmierczak PM, Reiser MF, Theisen D (2014) Non-contrast-enhanced MR angiography at 3 Tesla in patients with advanced peripheral arterial occlusive disease. PLoS One 9:e91078
31. Partovi S, Rasmus M, Schulte AC et al.(2013) ECG-triggered non-enhanced MR angiography of peripheral arteries in comparison to DSA in patients with peripheral artery occlusive disease. MAGMA 26:271-80

Figures

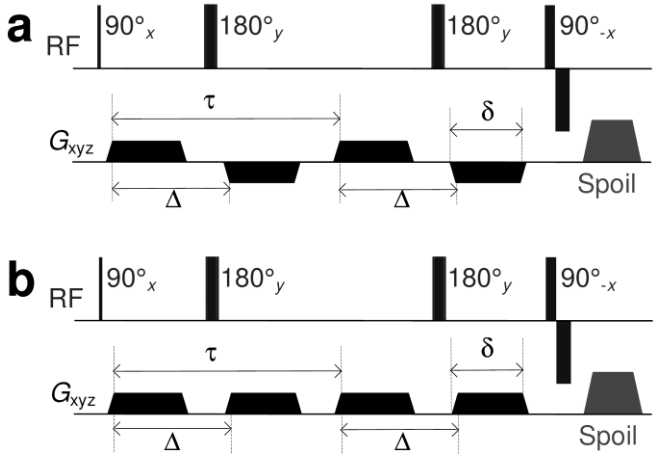

Fig. 1: flow-preparation modules for (a) velocity sensitization and (b) acceleration sensitization. The motion sensitization gradients (MSG) are the lower of the two lines.

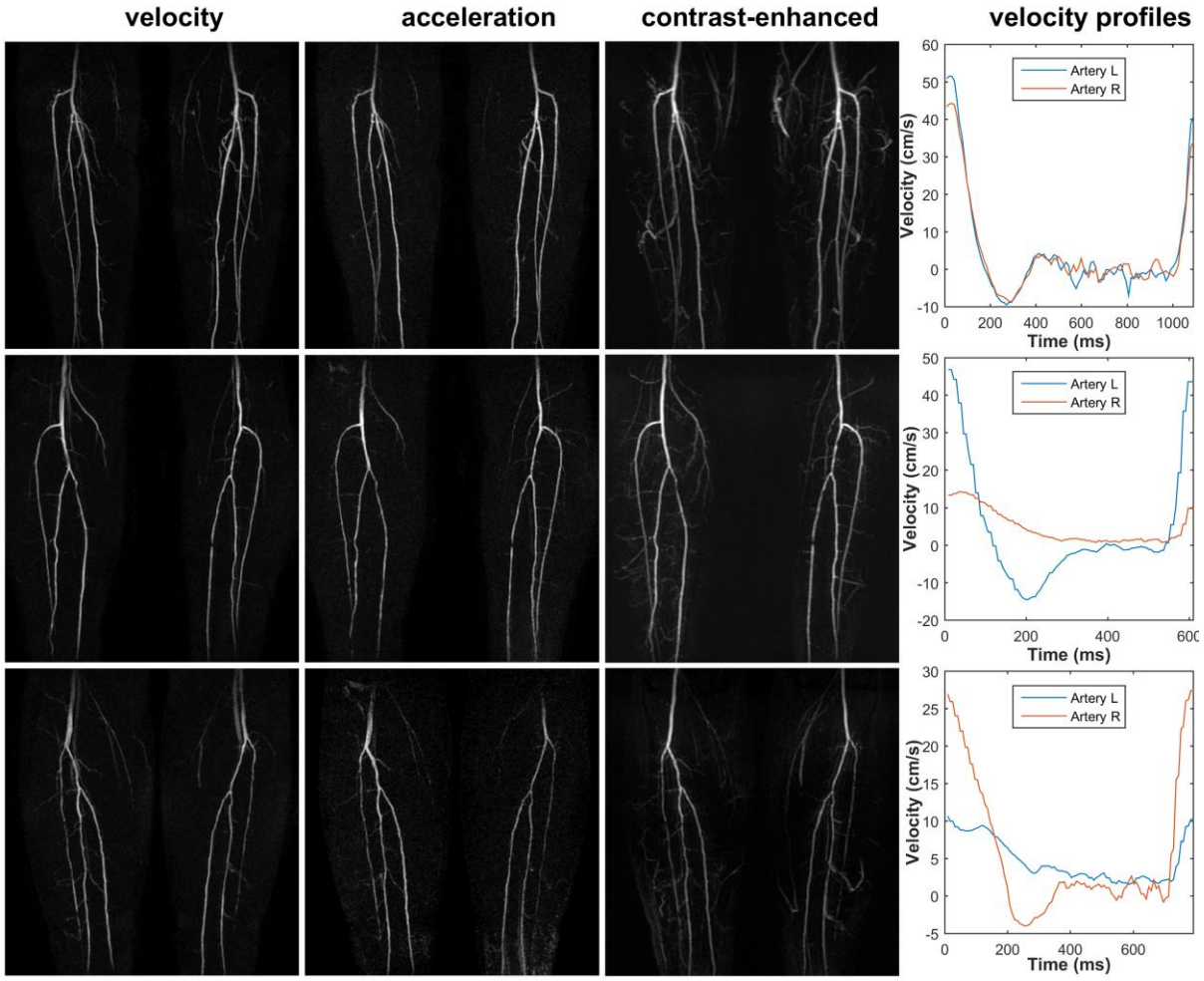

Fig. 2: Typical examples of velocity-dependent, acceleration-dependent, and contrast-enhanced MRA, images for three patients. The corresponding phase-contrast velocity profiles demonstrate flow is pulsatile in both legs, despite some differences between them.

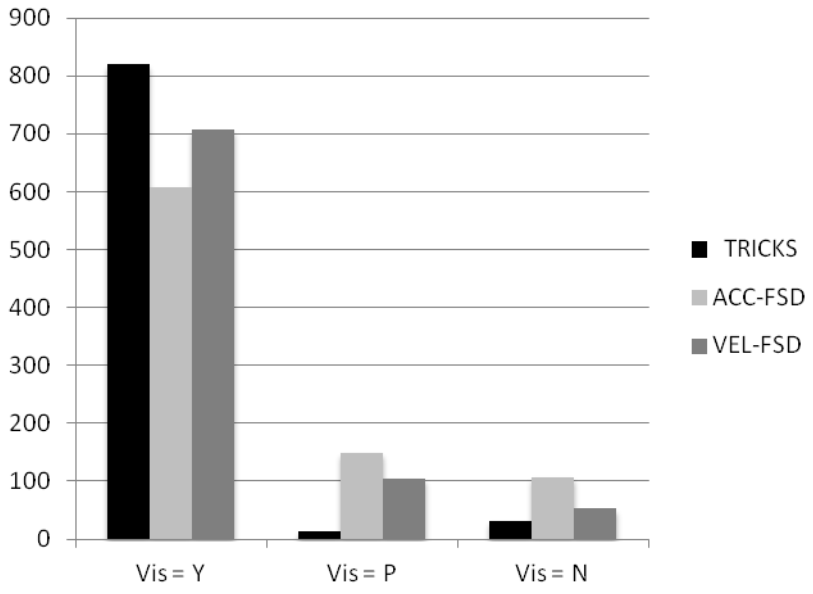

Fig.3: Segment visibility rating for each of the 3 techniques (864 segments in total for each technique – Y= yes, N=Not visible, P=Partially visible)

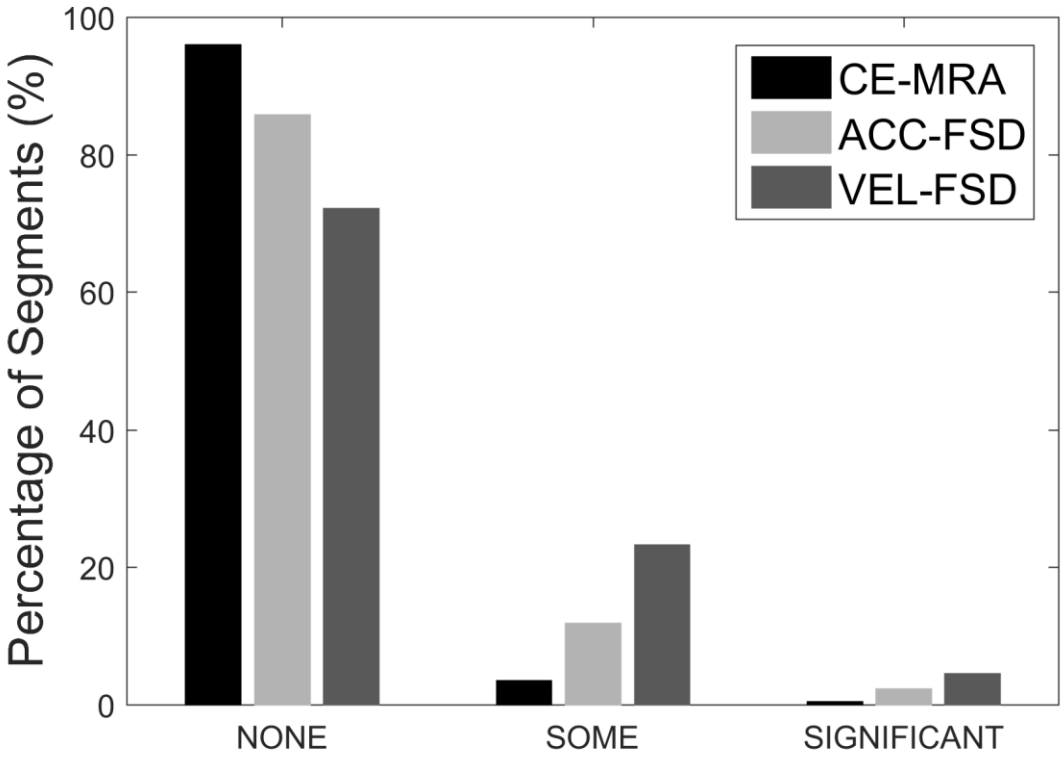

Fig. 4: Segment venous contamination rating for each technique.

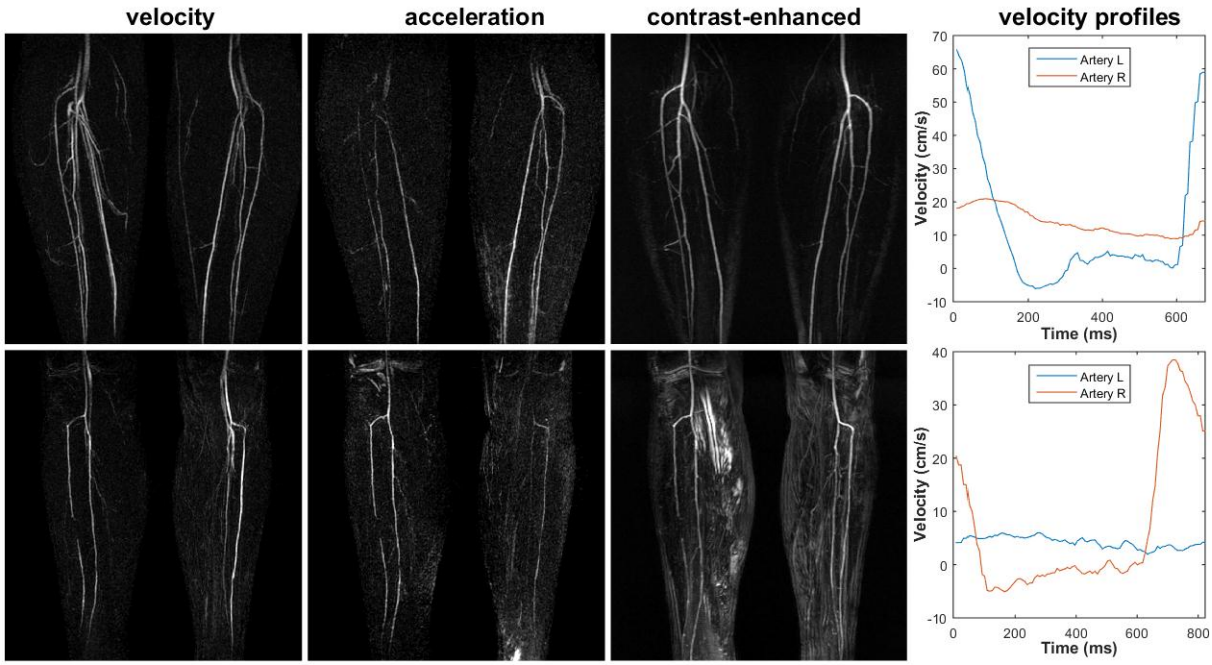

Fig. 5: Example images from cases with little acceleration in one leg, and poor acceleration-sensitized NCE-MRA from the corresponding leg. Velocity-dependent, acceleration-dependent, and contrast-enhanced MRA images are shown, with the phase-contrast velocity profiles demonstrating the lack of pulsatility in one leg.

Tables

Method	Prox Pop	Distal Pop	TPT	Prox AT	Distal AT	Prox Peroneal	Distal Peroneal	Prox PT	Distal PT
CE-MRA	99	99	99	99	99	98	98	98	98
ACC-FSD	47.9	63.5	81.3	86.5	86.5	87.5	87.5	87.5	86.5
VEL-FSD	83.3	93.8	94.8	94.8	91.7	93.8	88.5	91.7	90.6

Table 1: Percentage of segments with diagnostic confidence rated as moderate or high for each method by anatomical location (Proximal popliteal, Distal popliteal, Tibioperoneal trunk, Proximal anterior tibial, Distal anterior tibial, Proximal peroneal, Distal peroneal, Proximal posterior tibial, distal posterior tibial)

Method	Sensitivity (%)	Specificity (%)	PPV (%)	NPV (%)
ACC-FSD: per-segment	63.4	92.5	50.4	95.4
VEL-FSD: per-segment	65.3	92.7	52.5	95.6
ACC-FSD: per-limb	73	66.1	57.4	79.6
VEL-FSD: per-limb	87.2	61.4	60.7	87.5
ACC-FSD: per-patient	92	60.9	71.9	87.5
VEL-FSD: per-patient	96	43.5	64.9	90.9

Table 2: Calculated sensitivity and specificity of the two methods for significant disease (PPV - Positive predictive value, NPV - negative predictive value)